CFD Validations with FDA Benchmarks of Medical Devices Flows

Chien-Jung Huang, Iñaki Çaldichoury, Facundo Del Pin, Rodrigo R. Paz
LSTC

Abstract

Computational Fluid Dynamics (CFD) is a powerful tool and has been applied on various problems. In the biomedical application, CFD has been applied not only on the simulations of blood flow and airflow in lungs, but also on the designs and analysis of the medical devices. This study focuses on two benchmark problems proposed by FDA for the standardization of CFD simulation on the safety analysis on the blood-contacting medical devices, which is called CFD Round Robin study. The first case is the flow in a nozzle with a conical change in diameter at one end of the throat, and a sudden change at the other end, whereas the second problem is the system of blood pump housing and impeller. These two problems were simulated with the LS-DYNA® ICFD solvers and the obtained results are compared with results from other numerical and experimental studies.

Introduction

Computational fluid dynamics (CFD) is a powerful tool providing prediction and analysis of the flow fields. With the growing computational speed and development of the numerical algorithm, the capability of CFD on providing accurate and credible predictions has been enhancing nowadays. In the biomedical application, CFD has been applied not only on the simulations of blood flow and airflow in lungs, but also on the designs and analysis of the medical devices. Using numerical analysis on biomedical related problems can provide a clear understanding of the flow pattern and shear distribution in the flow field. Moreover, on the design and analysis of the blood-contacting medical devices, CFD can be a relatively cheap and fast option compared with the in-vitro bench-top investigations.

As to the evaluation of the safety of the blood-contacting devices, the ratio of hemolysis is an important factor. Hemolysis is a phenomenon of blood cell rupture, which happens due to long duration under large local shear stress [2]. Inside the medical devices, mechanical effects including changes in cross-section, working surfaces, and turbulence will enhance the occurrence of hemolysis. Under the transitional or turbulent flow regimes, the prediction of flow fields using the computational simulation can be sensitive to the simulation setup such as choice of turbulence models, boundary conditions, time integration schemes or mesh configuration. This indicates that it is crucial to select a proper numerical model in order to correctly estimate the ratio of hemolysis in the medical devices.

The United States Food and Drug Administration (FDA) have launched a Critical Path Initiative (CPI) [1] program to standardize the use of computational simulation on the design of the blood-contacting medical devices and analysis of the ratio of hemolysis in them. The goal of this project is to establish the guidelines for applying CFD on the evaluation and the optimization of the medical devices. FDA has proposed two benchmark problems [3] for CFD verification and validation. The first benchmark problem is the flow in a nozzle containing a gradual and sudden change of the diameter. The nozzle flows with different flowrates, which correspond to different flow regimes, are examined. The second study is the flow in a simplified centrifugal blood pump. The flow field under various pump operation conditions are analyzed. For each benchmark problem, the experimental results [4-6] and the flow field predicted with numerical simulations [7-10] from different institutes are collected. The comparison between results obtained using different numerical models are made and analyzed [11-12]. In this study, these two benchmark problems will be analyzed using LS-DYNA ICFD solver.

Methods

The simulations of blood flows in the nozzle with sudden expansion and pump proposed by FDA with different flow conditions are conducted and analyzed. The simulations are conducted using LS-DYNA ICFD incompressible flow solver under framework of finite element method and the second order fractional step time integration scheme. The fluid is assumed to be Newtonian with the same density and viscosity as blood, ρ= 1035 kg/m^3 and μ =3.5·10^{-3} N-s/m^2. The geometries and simulation setups are described in the following section:

Study 1: Nozzle Model

The proposed idealized nozzle model consists of four parts containing characteristics of some blood-conveying medical devices. There are inlet and outlet tubes with diameter 0.012 m and a nozzle throat with diameter 0.004 m. There is also a cone-shaped tube connecting the inlet tube with the nozzle throat (Figure 1). The flow will experience a gradual contraction of area from the inlet tube to the throat, then a sudden expansion of the area right after the throat to the outlet tube. The flows with Reynolds numbers 500, 2000 and 3500, corresponding to laminar, transitional, and turbulent flow regimes, will be analyzed, where as the flowrates are 5.21×10^{-6}, 2.08×10^{-5}, 3.64×10^{-5} (m^3/s) in these three flows. The Reynolds number is defined with the flow rate and the diameter at the throat. In the simulation, the length of the inlet is set to be 0.117 m and the length of the outlet tube is 0.18 m. The prescribed velocity profile is imposed at the inlet while the pressure is constant at outlet.

Under different flow conditions, different flow models and mesh sizes are used. At Re = 500, the flow is expect to be laminar. The parabolic velocity profile is set at the inlet. The domain is decomposed into approximately 2.25 million tetrahedron elements and with minimum mesh size 2.5×10^{-4} (m) in the throat. For the Re=2000 and 3500 cases, the Reynolds-averaged Navier–Stokes (RANS) k-ω standard model and Large Eddy Simulation (LES) Smagorinsky model are chosen for the transitional and turbulent flow regimes in the nozzle. The constant velocity profile is set at the inlet with 3% and 5% of turbulence intensity at Re = 2000 and 3500. With the LES Smagorinsky model, the Smagorinsky coefficient is set to be 0.1 empirically for flows in the pipe. Around 0.32 million elements are used in both cases, with minimum mesh size 2.5×10^{-4} (m) in the throat and maximum mesh size 1.0×10^{-3} (m) in the inlet and outlet tube. As to the k-ω standard model, the domain is decomposed into about 3.25 and 8.61 million elements, with minimum mesh size 2.0×10^{-4} (m) and 2.5×10^{-4} (m) in the throat, and maximum mesh size 5.0×10^{-4} (m) and 3.0×10^{-4} (m) in the outlet tube for Re=2000 and 3500 respectively.

In the simulations, the time step size is controlled so that the CFL number is always less or equal than 0.6. No effect of other body forces or gravity is applied.

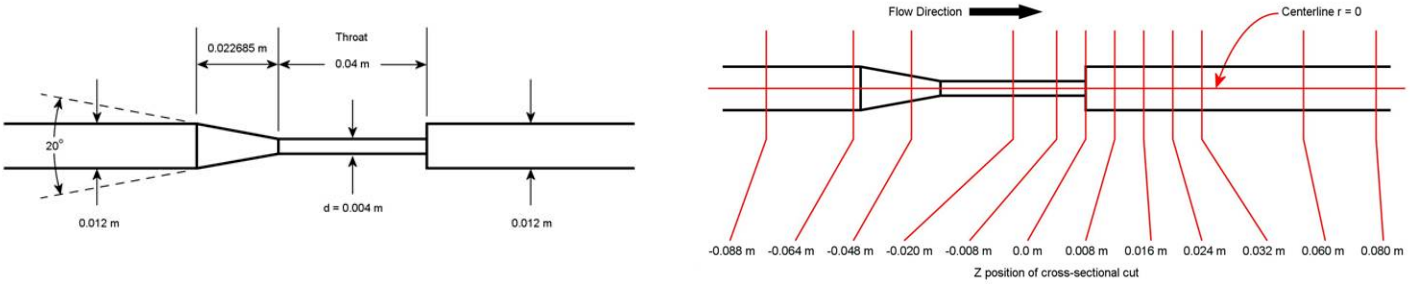

Figure 1: The dimension of the idealized nozzle model proposed by FDA (left). The flow direction and the definition of the axial coordinate z (right).

Study 2: Blood pump model

The simplified centrifugal pump geometry is shown in the Figure 2. The rotor is with diameter 52 mm and 4 mm thick. It has four 3 mm thick blades. The diameter of the inner chamber of the housing is 60 mm and the thickness is 9 mm. The clearances between the front and back of the impeller and the housing are 1 mm. The chamber is connected with a thraot at outlet, followed by a diffuser to the outlet tube with diameter 12 mm. The inlet curved tube also has the diameter 12 mm.

The flow field under two pump operation conditions with different flowrates and rotational speeds are simulated. In the first case, the flowrate Q = 2.5L/min and rotational speed 2500 RPM are set. While in the second case Q = 6L/min and 3500 RPM are chosen. The velocity distribution is prescribed at the inlet (Figure 2), where the velocity profiles are obtained from the experimental measurements using PIV at different operation conditions [3]. The pressure at the outlet is set to be constant, and the gravitational force is included. Since the goal is to predict the flow field after reaching steady state, instead of letting the rotor rotate during simulation, the non-inertial reference frame is applied on the fluid around the rotor. This is because the flow around the rotor at steady state can be analogue to flow experiencing constant angular velocity. Using non-inertial reference frame avoids mesh distortion and frequent remeshing due to rotation. For turbulence model, the LES Smagorinsky sub-grid scale model is employed, with 4% and 7% of turbulence intensity imposed at the inlet in the two cases. The simulation domain is decomposed into around 5.8 million tetrahedron elements as shown in Figure 3 in both cases. The time step size is controlled so that the CFL number is less or equal than 1.

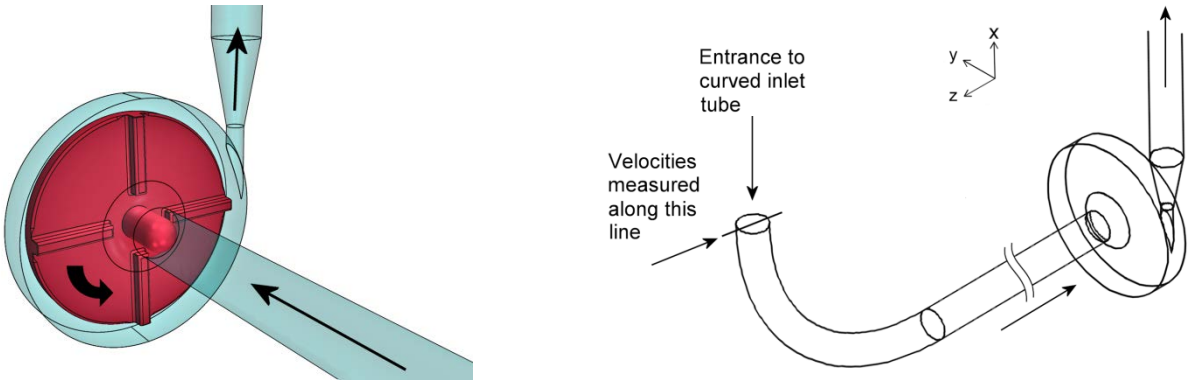

Figure 2: The geometry of the blood pump (left), and the location where the velocity is measured in the experiments the velocity profile is prescribed in the simulations (right) [1].

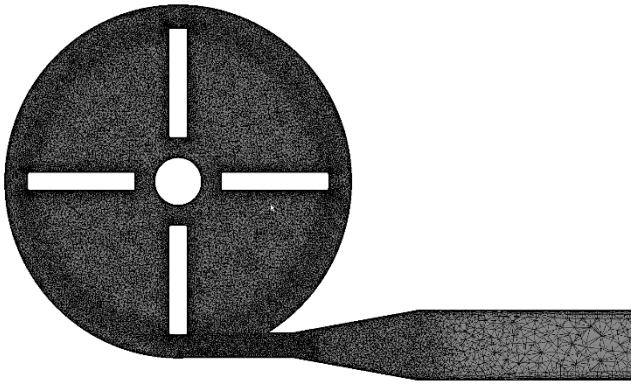

Figure 3: The mesh configuration used in the pump model on the plane which coincides to the mid-axis plane of the outlet diffuser.

Results

Study 1: Nozzle Model

At Re=500, the simulation results have a good agreement with the experimental results as shown in Figure 4. The axial velocity along the nozzle center line decreases gradually after the flow exiting the throat and forming a laminar jet (Figure 4(a)). The velocity distribution predicted by the ICFD solver in the throat (Figure 4(b)) and in the outlet tube (Figure 4(c)) matches well with the experimental data.

As to the transitional flow at Re = 2000, in the LES Smagorinsky model, the velocity of the jet decreases slower than experiments; while the jet breakdown location with k-ω standard model is earlier than the experimental data (Figure 5(a)). The velocity distributions from numerical prediction match with experimental results in the throat (Figure 5(b)), but result in a more smeared out jet velocity profile in the outlet tube (Figure 5(c)).

In terms of the turbulence jet flow at Re=3500, the flow fields obtained with the k-ω standard model is in accordance with the experimental data. The prediction by the LES Smagorinsky model, as in the results at Re=2000, shows a more gradual breakdown of the jet flow (Figure 7(a)). However, the velocity distributions along radial cuts by LES model still have a good agreement with the experiments in the throat as well as the in the outlet tube before the jet breakdown (Figure 7(a,b)). Figure 6 shows the obtained velocity magnitude distribution in the nozzle at steady state. The elongated jet structure predicted the LES model can be observed.

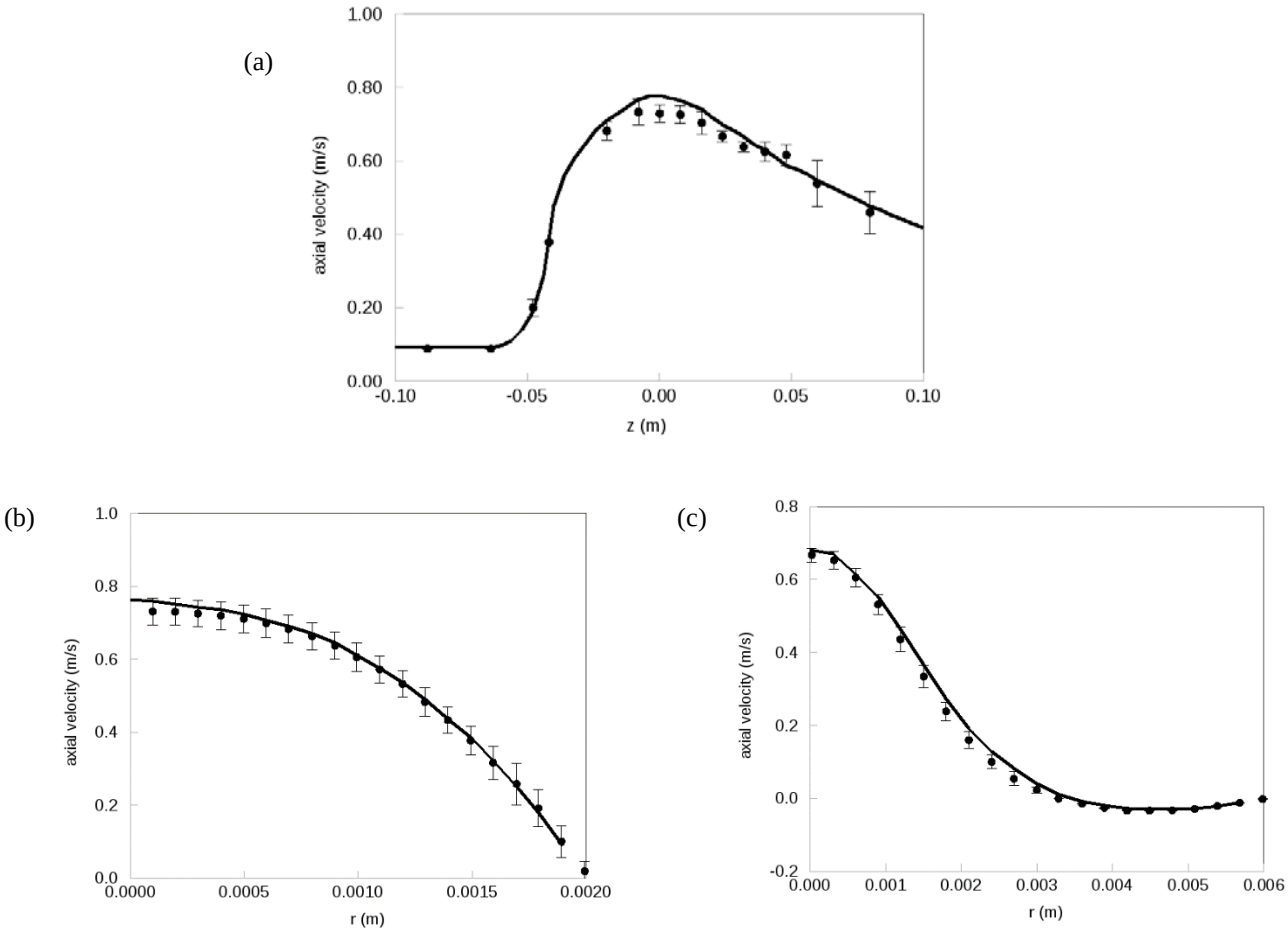

Figure 4: The distribution of the axial velocity in the nozzle along the center line (a), along radial direction at z = -0.008 (b) and at z = 0.024 (c) at steady state at Re=500. ●: Experiment [11]. Solid line: simulation.

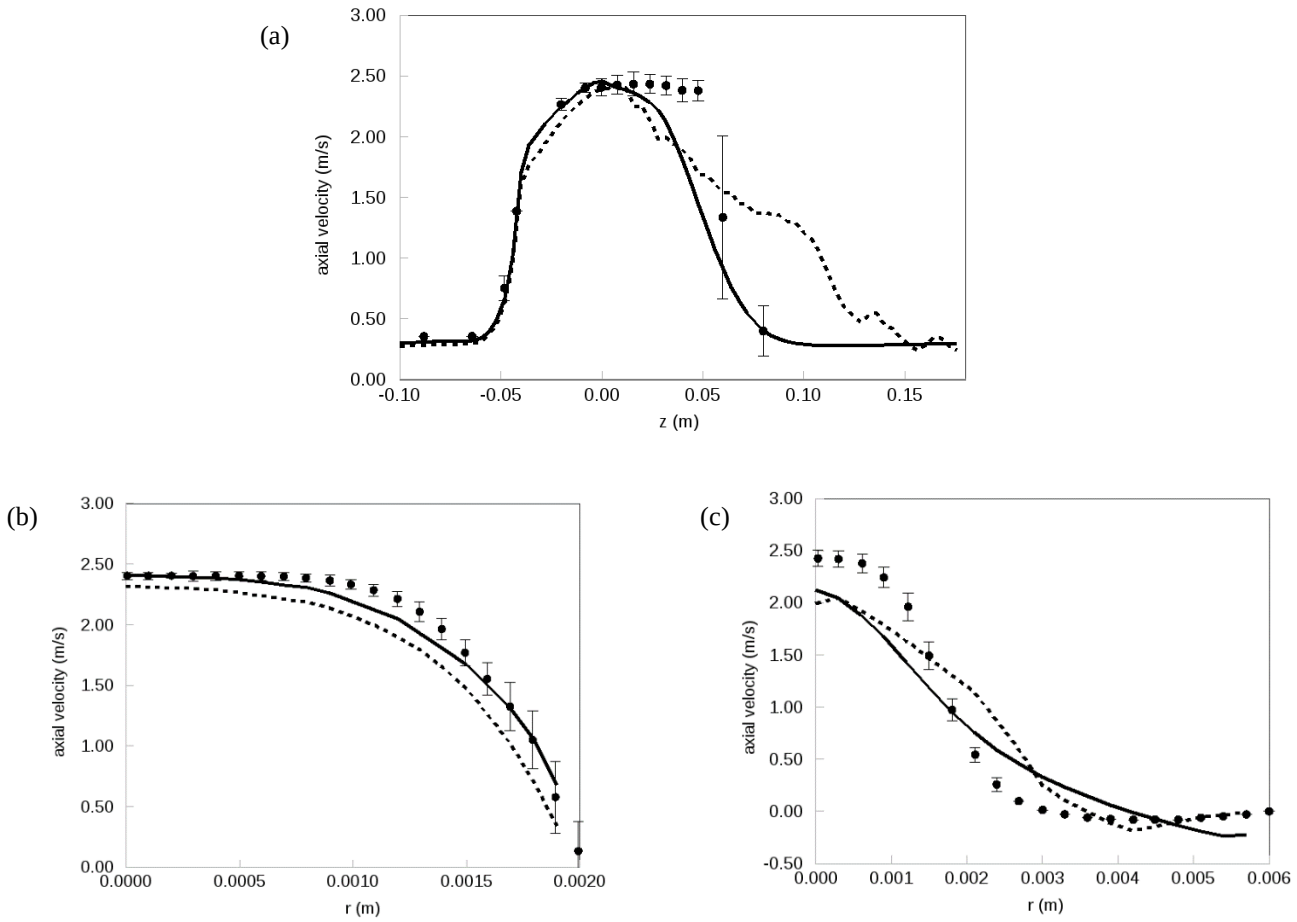

Figure 5: The distribution of the axial velocity in the nozzle along the center line (a), along radial direction at z = -0.008 (b) and at z = 0.032 (c) at steady state at Re=2000. The velocity shown is averaged within time interval 0.1 after reaching steady state. ●: Experiment [11]. Dashed line: LES Smagorinsky. Solid line: k-ω standard model.

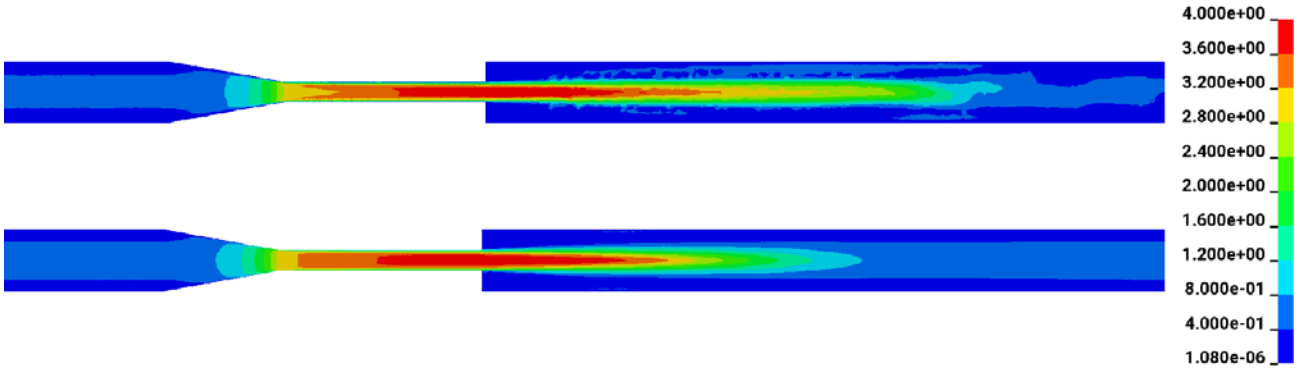

Figure 6: The magnitude of velocity field at steady state at Re = 3500 with LES (top) and k- ω (bottom) models.

Study 2: Blood pump model

In the simulation, the pump flow reaches steady state after about 20 rotations. The pressure differences across the pump under both operation conditions are lower than the pressure raises obtained from experiments

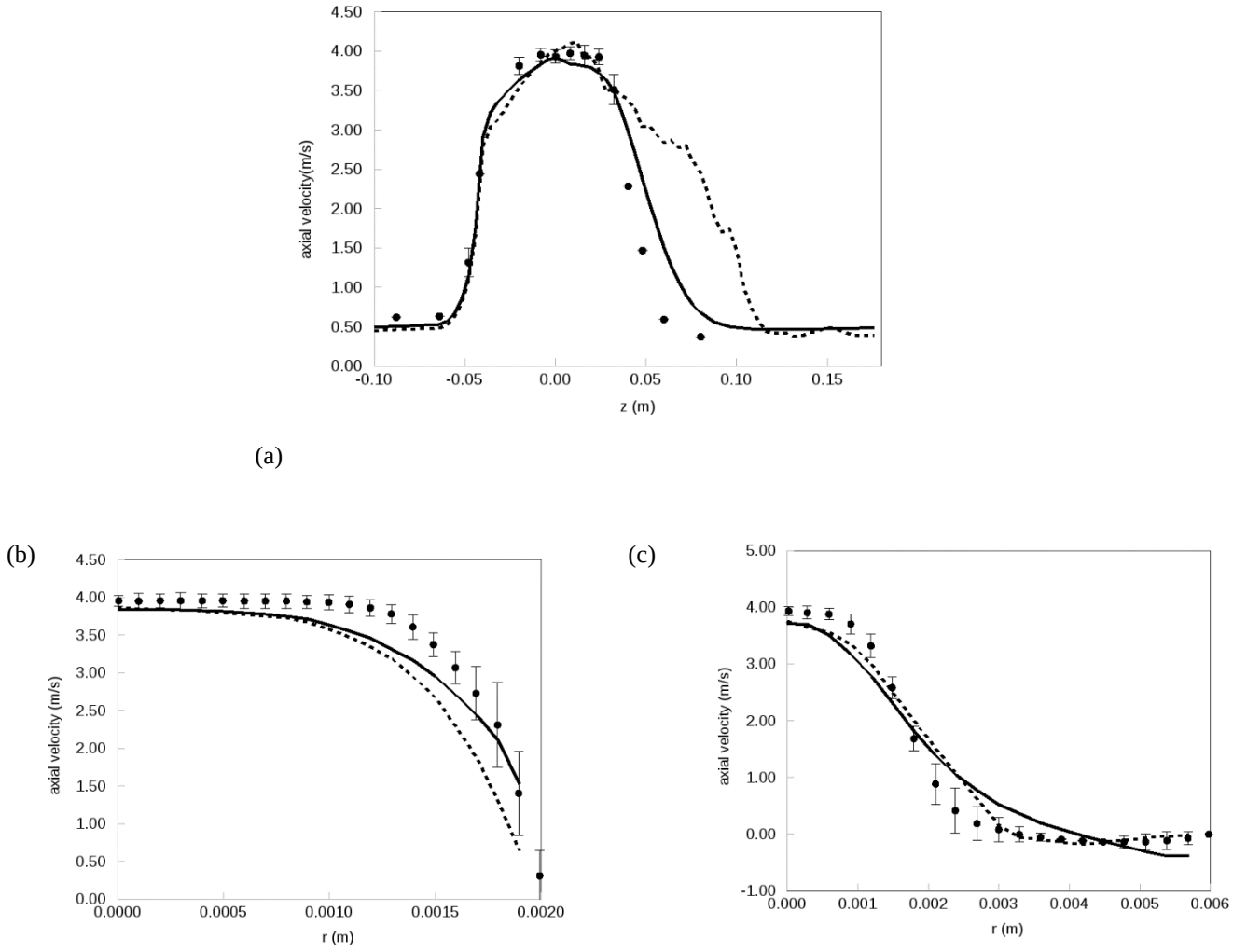

Figure 7: The distribution of the axial velocity in the nozzle along the center line (a), along radial direction at z = -0.008 (b) and at z = 0.024 (c) at steady state at Re=3500. The velocity shown is averaged within time interval 0.1 after reaching steady state. ●: Experiment [11]. Dashed line: LES Smagorinsky. Solid line: k-ω standard model.

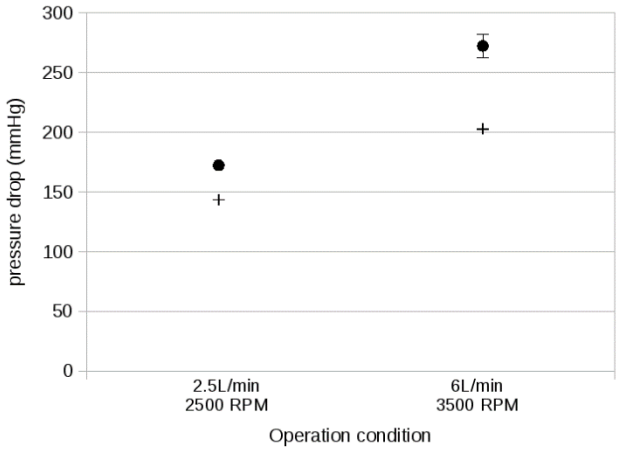

Figure 8: The comparison of the obtained Pressure drop across the blood pump at two pump operation conditions. ●: Experiment [12]. +: Present work.

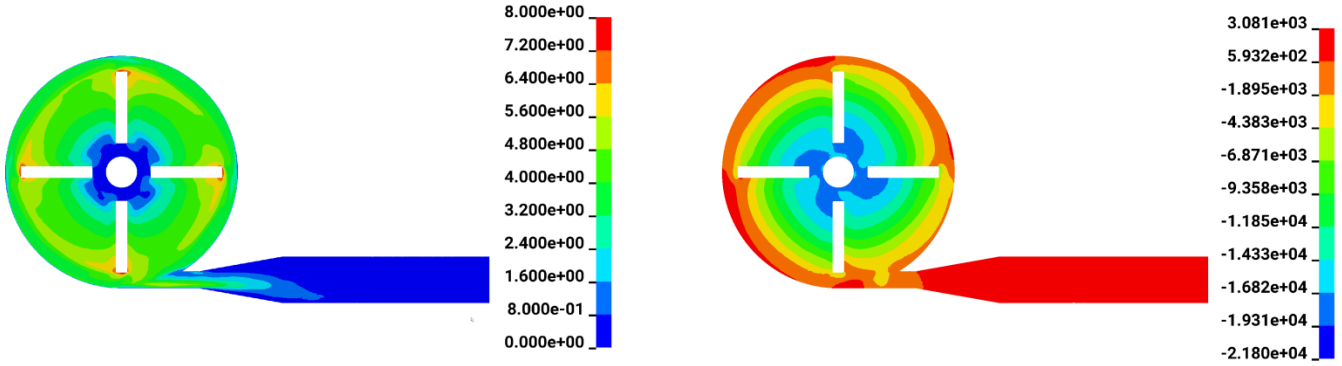

Figure 9: The magnitude of velocity (left) and pressure (right) distribution at steady state in flowrate 2.5L/min and rotational speed 2500 RPM.

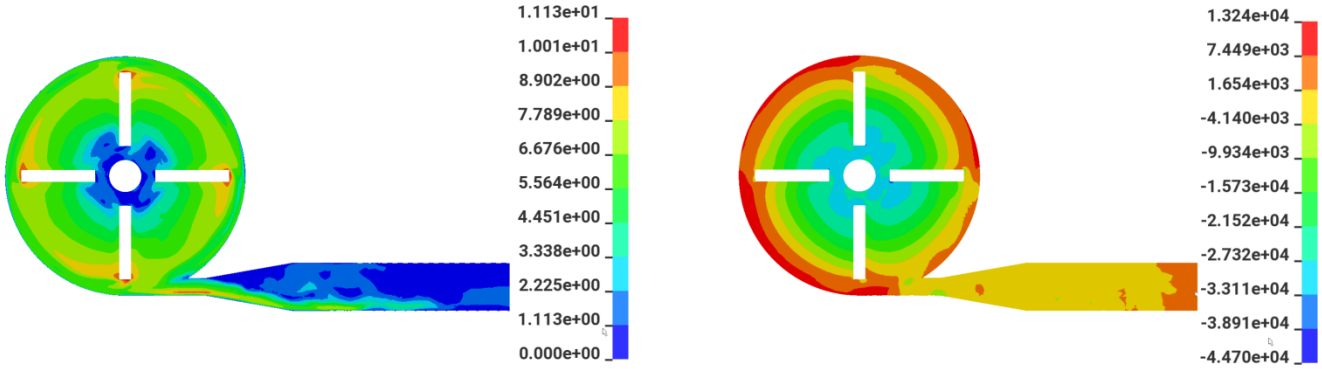

Figure 10: The magnitude of velocity (left) and pressure (right) distribution under flowrate 6L/min and rotational speed 3500 RPM.

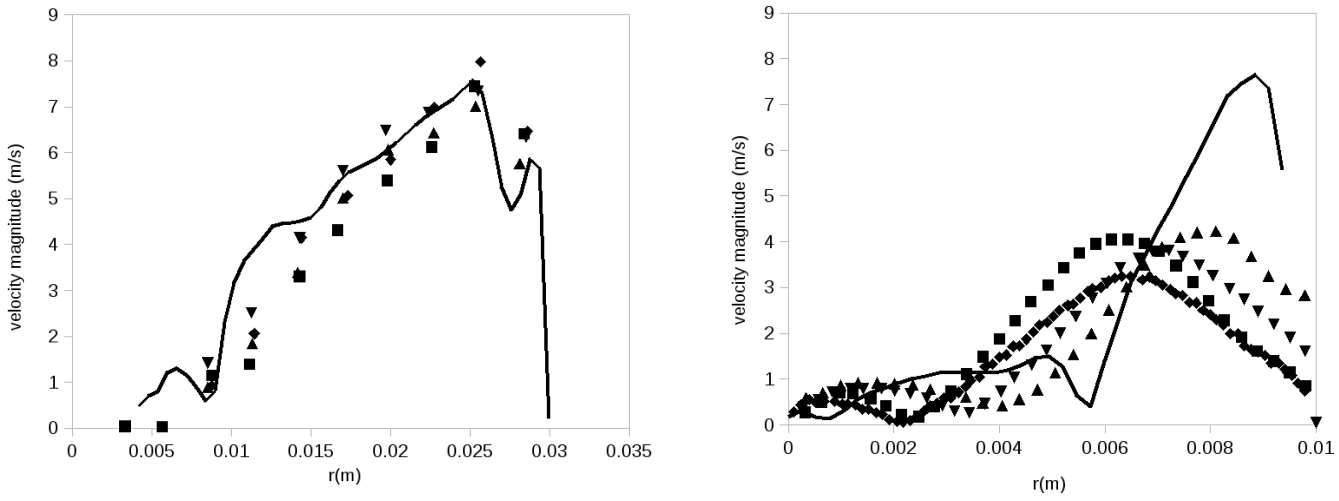

Figure 11: The magnitude of the two-dimensional velocity on the xy-plane passing the mid-axis plane of the outlet diffuser with experiment and simulation results in flowrate 6L/min and rotational speed 3500 RPM. Left: along the radial direction from the rotor center in the housing. Right: along the in the outlet diffuser. ▼▲■♦: experiments [12]. Solid line: present work.

(Figure 8). Figure 11 shows the distributions of the two-dimensional velocity on the xy-plane passing through the mid-axis plane of the outlet diffuser. The obtained velocity distribution between the blades has a good agreement with the experiments. However, the magnitude of the detached jet in the outlet diffuser appears to be larger compared with experiments.

Conclusions

In this work, the simulations of flow in the idealized blood nozzle and blood pump are successfully conducted with LS-DYNA ICFD solver. In the nozzle flow simulations, the obtained laminar nozzle flow field matches with the experimental results. For the transitional and turbulent regimes, the flow fields predicted by k-ω standard model show a good agreement with the flow fields from experiments. On the other hand, the LES Smagorinsky model predicts the jet breakdown locations to be more downstream. As to the pump flow, the qualitative trend of the obtained results matches with the experimental findings. The predicted pressure drops are lower than those from experiments in both operation conditions, and a larger velocity magnitude of the detached jet in diffuser is observed. The reason of the discrepancies may be from the use of LES Smagorinsky model, which is found to be more dissipative in transitional flows [13]. Furthermore, the Smagorinsky coefficient used in the model is determined empirically. Better numerical predictions may be obtained after the optimization of the Smagorinsky coefficients for these two problems.

References

[1] FDA's Critical Path Initiative https://www.fda.gov/scienceresearch/specialtopics/criticalpathinitiative/default.htm
[2] Blackshear Jr, P. L., Dorman, F. D., & Steinbach, J. H. (1965). Some mechanical effects that influence hemolysis. ASAIO J,11:112–7.
[3] FDA's "Critical Path" Computational Fluid Dynamics (CFD)/Blood Damage Project: Computational Round Robin problems https://nciphub.org/wiki/FDA_CFD
[4] Hariharan, P., Giarra, M., Reddy, V., Day, S. W., Manning, K. B., Deutsch, S., Hariharan, P., Giarra, M., Reddy, V., Day, S.W., Manning, K.B., Deutsch, S., Stewart, S.F., Myers, M.R., Berman, M.R., Burgreen, G.W. and Paterson, E.G. (2011). Multilaboratory particle image velocimetry analysis of the FDA benchmark nozzle model to support validation of computational fluid dynamics simulations. Journal of Biomechanical Engineering, 133(4), 041002.
[5] Herbertson, L. H., Olia, S. E., Daly, A., Noatch, C. P., Smith, W. A., Kameneva, M. V., & Malinauskas, R. A. (2015). Multilaboratory Study of Flow-Induced Hemolysis Using the FDA Benchmark Nozzle Model. Artificial organs, 39(3), 237-248.
[6] Giarra, M. N. (2009). Shear Stress Distribution and Hemolysis Measurements in a Centrifugal Blood Pump. Rochester Institute of Technology.
[7] Zmijanovic, V., Mendez, S., Moureau, V., & Nicoud, F. (2017). About the numerical robustness of biomedical benchmark cases: Interlaboratory FDA's idealized medical device. International journal for numerical methods in biomedical engineering, 33(1).
[8] Hariharan, P., D'Souza, G. A., Horner, M., Morrison, T. M., Malinauskas, R. A., & Myers, M. R. (2017). Use of the FDA nozzle model to illustrate validation techniques in computational fluid dynamics (CFD) simulations. PloS one, 12(6), e0178749.
[9] Nassau, C. J., Wray, T. J., & Agarwal, R. K. (2015, July). Computational Fluid Dynamic Analysis of a Blood Pump: An FDA Critical Path Initiative. In ASME/JSME/KSME 2015 Joint Fluids Engineering Conference (pp. V002T26A002-V002T26A002). American Society of Mechanical Engineers.
[10] Heck, M. L., Yen, A., Snyder, T. A., O'Rear, E. A., & Papavassiliou, D. V. (2017). Flow-Field Simulations and Hemolysis Estimates for the Food and Drug Administration Critical Path Initiative Centrifugal Blood Pump. Artificial organs, 41(10).
[11] Stewart, S. F., Paterson, E. G., Burgreen, G. W., Hariharan, P., Giarra, M., Reddy, V., Stewart, S.F., Paterson, E.G., Burgreen, G.W., Hariharan, P., Giarra, M., Reddy, V., Day, S.W., Manning, K.B., Deutsch, S., Berman, M.R. and Myers, M.R. (2012). Assessment of CFD performance in simulations of an idealized medical device: results of FDA's first computational interlaboratory study. Cardiovascular Engineering and Technology, 3(2), 139-160.
[12] Malinauskas, R. A., Hariharan, P., Day, S. W., Herbertson, L. H., Buesen, M., Steinseifer, U., Aycock, K.I., Good, B.C., Deutsch, S., Manning, K.B. and Craven, B.A. (2017). FDA benchmark medical device flow models for CFD validation. ASAIO Journal, 63(2), 150-160.
[13] Vreman, B., Geurts, B., & Kuerten, H. (1997). Large-eddy simulation of the turbulent mixing layer. *Journal of Fluid Mechanics*, *339*, 357-390.